Received: 2 November 2020 | Revised: 16 February 2021 | Accepted: 24 February 2021

DOI: 10.1096/fba.2020-00110

RESEARCH ARTICLE

FASEB BioAdvances WILEY

Lineage tracing of Foxd1-expressing embryonic progenitors to assess the role of divergent embryonic lineages on adult dermal fibroblast function

John T. Walker[1] | **Lauren E. Flynn**[1,2] | **Douglas W. Hamilton**[1,3]

[1]Department of Anatomy and Cell Biology, Schulich School of Medicine and Dentistry, The University of Western Ontario, London, Ontario, Canada

[2]Department of Chemical and Biochemical Engineering, Thompson Engineering Building, The University of Western Ontario, London, ON, Canada

[3]Division of Oral Biology, Schulich School of Medicine and Dentistry, The University of Western Ontario, London, ON, Canada

Correspondence
Douglas W. Hamilton, PhD, Division of Oral Biology, Schulich School of Medicine and Dentistry, The University of Western Ontario, Dental Sciences Building, London, Ontario, N6A 5C1.
Email: dhamil2@uwo.ca

Abstract

Recent studies have highlighted the functional diversity of dermal fibroblast populations in health and disease, with part of this diversity linked to fibroblast lineage and embryonic origin. Fibroblasts derived from *foxd1*-expressing progenitors contribute to the myofibroblast populations present in lung and kidney fibrosis in mice but have not been investigated in the context of dermal wound repair. Using a Cre/Lox system to genetically track populations derived from *foxd1*-expressing progenitors, lineage-positive fibroblasts were identified as a subset of the dermal fibroblast population. During development, lineage-positive cells were most abundant within the dorsal embryonic tissues, contributing to the developing dermal fibroblast population, and remaining in this niche into adulthood. In adult mice, assessment of fibrosis-related gene expression in lineage-positive and lineage-negative populations isolated from wounded and unwounded dorsal skin was performed, identifying an enrichment of transcripts associated with matrix synthesis and remodeling in the lineage-positive populations. Using a novel excisional wound model, ventral skin healed with a greatly reduced frequency of *foxd1* lineage-positive cells. This work supports that the embryonic origin of fibroblasts is an important predictor of fibroblast function, but also highlights that within disparate regions, fibroblasts of different lineages likely undergo convergent differentiation contributing to phenotypic similarities.

KEYWORDS

fibroblast heterogeneity, lineage tracing, myofibroblasts, wound healing

1 | INTRODUCTION

Within the skin, resident fibroblasts have long been proposed as the primary source of myofibroblasts during cutaneous wound repair.[1] Recent evidence from lineage tracing studies in mice has supported this hypothesis,[2,3] while other research has demonstrated complementary myofibroblast contribution from perivascular cells, adipocytes, and bone marrow-derived populations in skin fibrosis and wound healing.[4-6] Myofibroblasts, characterized by the expression of alpha smooth muscle actin (αSMA), are the main source of extracellular matrix (ECM) production during tissue injury.[7,8]

Abbreviations: FLN, *Foxd1*-lineage negative; FLP, *Foxd1*-lineage positive.

This is an open access article under the terms of the Creative Commons Attribution-NonCommercial License, which permits use, distribution and reproduction in any medium, provided the original work is properly cited and is not used for commercial purposes.
© 2021 The Authors. *FASEB BioAdvances* published by the Federation of American Societies for Experimental Biology

As such, investigation into the progenitors from which these myofibroblast populations originate within the skin during health and disease may provide insight into novel strategies to both improve wound healing and treat skin fibrosis.[9,10]

An important finding from murine lineage tracing studies is that there is previously unrecognized heterogeneity within fibroblast populations, and that this heterogeneity is correlated with specific gene expression signatures in their associated embryonic precursor populations.[2,3,9,10] During development, the most dorsal fibroblast population, characterized by the expression of *blimp1* and *lrig1*, gives rise to the papillary dermal fibroblasts of postnatal mice.[3] In contrast, the more ventral population, expressing *dlk1*, contributes to the reticular dermal fibroblasts and underlying adipogenic populations.[3,11] Furthermore, lineage tracing analysis of these populations identified their unique contributions to dermal wound repair in adult mice. While the *dlk1*-traced lower dermis contributed to early granulation tissue formation, the upper *blimp1*-traced population migrated into the wound during reepithelialization, and was determined to be critical for hair follicle formation.[3]

Further investigation of embryonic lineages identified that different fibroblast subsets have distinct specializations that may contribute to their roles in granulation tissue formation. Tracing a population of fibroblasts characterized by embryonic expression of *engrailed-1*, Rinkevich et al. identified a subset of fibroblasts with greater fibrogenic potential relative to fibroblasts derived from precursors not expressing *engrailed-1*.[2] More importantly, in this study, the cell surface marker and enzyme CD26 (Dipeptidyl peptidase-4; Dpp4) was enriched on adult mouse fibroblasts of the fibrogenic *engrailed-1* lineage. In adult mice, wounds treated with a chemical inhibitor of Dpp4 healed slower but had a significant reduction in scar size, highlighting the translational potential of this research.[2]

The level of heterogeneity within dermal fibroblast populations has recently been assessed in human skin using single-cell RNA-seq analyses.[12,13] These studies have identified approximately five subpopulations of fibroblasts based on cluster analysis of gene expression profiles. Whether these populations are fixed, and predetermined based on developmental lineage, or if cells from one discrete subtype can transition to another, are critical questions arising from these studies with important clinical implications. Lineage tracing studies in mice represent a promising tool to explore these important questions.

In fibrotic processes including dermal wound healing and organ fibrosis, myofibroblasts are implicated as the primary effector cell of uncontrolled matrix deposition across organs, independent of their origins.[14,15] However, recent lineage tracing studies have also demonstrated that unique embryonic gene signatures within dermal fibroblast precursors can be predictive of distinct myofibroblast functions during dermal wound repair in adulthood.[2,3] Building from previous work, binary expression of *foxd1* during embryogenesis presented a new potential marker to be investigated within the skin. *Foxd1* is a transcription factor expressed primarily during development, and has been shown to be required for the appropriate differentiation of stromal cell progenitors within the kidney.[16,17] Notably, resident *foxd1* lineage-derived populations in the kidney and lung have been shown to contribute to the myofibroblast populations in induced renal fibrosis following unilateral ureteral obstruction and ischemia reperfusion injury, as well as bleomycin-induced lung fibrosis, respectively.[18,19]

In the present study, expression of *foxd1* by embryonic dermal progenitors was probed using a Cre/Lox lineage tracing system, identifying *foxd1*-expressing progenitors as the source of a subset of dermal fibroblasts. It was further determined that *foxd1* expression was highly restricted in adult dermal tissue. Thus, lineage tracing of *foxd1*-expressing progenitors provided a system with which to track two embryonically distinct fibroblast lineages, those derived from *foxd1*-expressing progenitors, and those derived from alternative progenitor populations. Using this strategy, the effect of embryonic lineage on adult fibroblast function was probed with the *foxd1*-lineage hypothesized to contribute to the more fibrogenic dermal fibroblast subsets that have been previously described.[2,3] Finally, during the characterization of $foxd1^{+}$ progenitor-derived fibroblasts, it was noted that these cells were primarily confined to the dorsal dermis, making up a relatively small fraction of dermal fibroblasts in the ventral skin. Based on the unique distribution of these populations between dorsal and ventral skin, pilot studies were performed using a novel excisional wound healing model to probe healing in dorsal versus ventral skin to assess whether these lineage differences resulted in altered tissue repair.

2 | MATERIALS AND METHODS

2.1 | Mice

All animal procedures were in compliance with the Canadian Council on Animal Care (CCAC) guidelines and all protocols were reviewed and approved by the Animal Care Committee at Western University. *Foxd1GC (Foxd1*$^{tm1(GFP/Cre)Amc/J}$), *Foxd1GCE(B6;129S4-Foxd1*$^{tm2(GFP/Cre/ERT2)Amc/J}$), *Ai14(B6.Cg-Gt(ROSA)26Sor*$^{tm14(CAG-tdTomato)Hze/J}$), and *mTmG (B6.129(Cg)-Gt(ROSA)26Sor*$^{tm4(ACTB-tdTomato,-EGFP)Luo/J}$) mice were purchased from The Jackson Laboratory (Farmington, CT), and genotyped as per their instructions. Mice that were heterozygous for the alleles of interest were used for all experiments. For timed pregnancy, females were monitored for vaginal plugs and the day following initial detection was considered embryonic day 0.5 (E0.5). Embryos were isolated from pregnant females at E9.5,

E10.5, E11.5, E14.5, and E17.5 as specified for each experiment. For all-time points, at least three embryos were analyzed from at least two independent litters.

2.2 | Tamoxifen injections

To temporally control Cre-mediated recombination, mice carrying a tamoxifen-inducible Cre variant, CreER^{T2}, were crossed to *Ai14* reporter mice.[20,21] Using this strategy, injection of tamoxifen was used to determine the temporal expression of *Foxd1* in both embryonic and adult tissues.

For the developmental studies, timed pregnancies were used for the embryo isolations as described above. In these animals, tamoxifen was injected intraperitoneally into pregnant females twice on 2 consecutive days at a dose of 0.6 mg per day. For all studies, a solution of 10 mg/ml tamoxifen in 90% corn oil (Sigma-Aldrich, Oakville, ON, Canada) and 10% ethanol was administered. A minimum of three embryos from one or more litters were analyzed at all-time points.

Tamoxifen injection in postnatal mice was performed on mice heterozygous for both *Foxd1GCE* and *Ai14* alleles. At 1 month of age, mice were injected with 1 mg of tamoxifen each day for 3 consecutive days. At 2 months of age, wounding experiments were performed using a non-splinted wound model as previously described.[22] Briefly, mice were anesthetized with Ketamine (90 mg/kg) and Xylazine (5 mg/kg). The dorsal skin of mice was shaved, and hair was removed with depilating cream (Nair®, Church and Dwight; Mississauga, ON, Canada). Two full-thickness dorsal wounds were made with a 6 mm biopsy punch (Integra™ Miltex™). Wounds were left to heal without bandaging. Pain was managed using 0.05 mg/kg buprenorphine administered intraperitoneally prior to surgery and again 6–8 hours following surgery. Directly following wounding, mice were subjected to a second tamoxifen regimen of 1 mg each day for 3 consecutive days. After 7 days post wounding, the animals were euthanized, and tissues were collected for histological analyses. Postnatal tamoxifen injection and wounding were performed on six animals. Tissues from these animals were compared to unwounded adult skin, and granulation tissue at 7 days post wounding (non-splinted) from constitutively active *Foxd1GC*/*Ai14* mice.

2.3 | Dorsal wound healing

Dorsal wound healing experiments conducted for histological analysis and cell isolations using Foxd1*GC*/Ai14 mice were performed as above, but were also splinted and wrapped as described previously.[23] A splinted wound model was used to impair rapid wound contraction, necessitating closure through granulation tissue formation and remodeling. The dorsal skin was shaved, and the remaining hair was removed with depilating cream. The 6 mm wounds were created with a biopsy punch and wounds were splinted open with silicone splints (Grace Bio labs; Bend, ORE, USA), which were held in place with a cyanoacrylate adhesive and 6–0 nylon sutures. Wounds were then covered with an adhesive contact layer (Mepitel® One; Mölnlycke; Gothenburg, Sweden) and a semiocclusive dressing (OPSITE®; Smith & Nephew; Mississauga, ON, Canada), prior to being wrapped in a self-adherent bandage and cloth tape. Following surgery, pain was controlled using 0.05 mg/kg buprenorphine delivered intraperitoneally prior to surgery and 6–8 hours following surgery. Dressings were changed every 3–4 days. For the 21-day time point, bandages and splints were removed after 14 days, at which time the wounds had reepithelialized.

2.4 | Histology and immunofluorescence microscopy analyses

Isolated embryos, skin, and wound tissue were fixed in 10% of neutral-buffered formalin for 24 hours at 4ºC. These tissue samples were then dehydrated in a sucrose gradient prior to embedding in frozen section compound (Leica, Wetzlar, Germany). Samples were frozen on dry ice and were stored at −20ºC. Cryosections were cut to 8 μm thickness. Unstained sections used to investigate endogenous fluorescent proteins were washed in phosphate-buffered saline (PBS) and directly mounted with VectaShield mounting media with DAPI (Vector Labs; Burlington, ON, Canada). For antibody labeling, slides were first washed with 1% of sodium dodecyl sulfate for 5 minutes, rinsed three times in PBS, and incubated for 30 minutes in 10% of horse serum in PBS for blocking. Sections were then incubated with primary antibodies as outlined in Table 1 in 10% of horse serum. Following staining, slides were labeled with VectaShield mounting media with DAPI. Negative

TABLE 1 Antibodies used for histological assessment

Target	Tissue investigated	Antibody ID	Dilution
αSMA	Adult	Ab5694 (Abcam)	1:100
CD26	Adult	AF954 (R&D systems)	1:50
GFP	Embryonic/Adult	Ab6673 (Abcam)	1:200
PDGFRα	Adult	AF1062 (R&D systems)	1:100
PDGFRβ	Adult	AF1042 (R&D systems)	1:50
CD31	Adult	Ab28364 (Abcam)	1:200
Vimentin	Adult	Ab92547 (Abcam)	1:500

controls lacking primary antibodies were included for all antibody labeling to gate out background autofluorescence and confirm staining specificity.

2.5 | Dermal fibroblast isolation

To isolate dermal fibroblasts from wounded and subject-matched healthy tissue, skin was excised from *Foxd1GC/Ai14* mice 10 days post wounding using an 8 mm biopsy punch centered on the middle of the wound, or excised from unwounded, depilated dorsal skin outside of the wounded area. For isolation of naïve healthy fibroblasts for culture studies, unwounded mice were depilated, and the dorsal skin was removed immediately. In all cases, subcutaneous fat was mechanically removed from the skin. The full, excised dorsal skin was then incubated in 0.25% of trypsin with 100 μg/ml dispase for 30 minutes at 37ºC. The epidermis was then removed mechanically by scraping the surface with a scalpel blade, and the remaining dermis was minced with a scalpel. The minced tissue was incubated in a digest solution of 4 mg/ml collagenase IV (Gibco; Thermo Fisher Scientific; Mississauga, ON, Canada) in DMEM/Ham's F-12 media for 2 hours, at 37ºC on a shaker set to 100 rpm. The resultant cell suspension was filtered through 100 μm and 40 μm nylon filters and prepared for fluorescence-activated cell sorting (FACS). Individual samples were processed independently from wounded and unwounded tissue. For isolation of naïve healthy fibroblasts, cells from 4 to 6 mice were pooled.

2.6 | Fluorescence-activated cell sorting

Cell suspensions were stained with LIVE/DEAD fixable aqua stain (Thermo Fisher Scientific; Mississauga, ON, Canada), as per the manufacturer's instructions. Cells were then incubated on ice for 25 minutes with APC-labeled antibodies for CD31 (BD Pharmingen; 551262, San Jose, CA, USA), CD45 (BD Pharmingen; 559864), and EpCAM (BD Pharmingen; 563478), each diluted 1:25 in PBS with 5% of FBS, to exclude endothelial, hematopoietic, and epithelial populations, respectively. Cells were then sorted on a FACSAria III cell sorter as follows: Forward- and side-scatter were first used to select individual cells. Using a 405 nm laser with a 510/50 filter, cells negative for the LIVE/DEAD fixable aqua stain were selected. Next, using a 633 nm laser with 660/20 filter, cells negative for APC were selected. Finally, the remaining fibroblast populations were sorted into the *Foxd1*-lineage positive (FLP) and *Foxd1*-lineage negative (FLN) subpopulations based on expression of tdTomato using a 561 nm laser with 610/20 filter.

2.7 | Cell culture

To assess isolated cells in culture, free-floating soft collagen gels were used as a three-dimensional culture substrate. For these studies, 2 mg/ml collagen gels were synthesized by neutralizing 6 mg/ml collagen (Nutragen; Advanced Biomatrix; Carlsbad, CA) with HEPES (final concentration 0.02 M). This solution was then combined with FACS-sorted fibroblasts in culture media. For each 500 μl collagen gel, 70,000 cells were seeded using a 24-well suspension culture plate as a mold. The samples were incubated for 30 minutes at 37ºC to allow gelation and then detached from the well plate with a pipette tip. Samples were cultured in DMEM/Ham's F-12 media supplemented with penicillin/streptomycin and 10% of FBS. To induce a myofibroblast phenotype, one set of samples was treated with 5 ng/ml mouse TGFβ1 (R&D Systems; Minneapolis, MN, USA) and another set was left untreated as controls. Depending on the cell yield, 1–3 collagen gels were synthesized per treatment group for each cell lineage. After 16 hours, the cells were cultured in DMEM/Ham's F-12 media supplemented with 5% of FBS, with fresh TGFβ1 added daily, for a total of 7 days. On day 7, the gels were digested in 4 mg/ml collagenase type IV in DMEM/Ham's F-12 media for RNA isolation. Multiple gels from the same group were pooled. These cell culture experiments were performed on isolated cells from a total of six independent digestions, each combining the pooled fibroblasts from 4 to 6 mice.

2.8 | RNA isolation

RNA was isolated from freshly sorted FLP and FLN fibroblast populations and from cells cultured in collagen gels. For all samples, RNA was isolated with TRIzol reagent (Thermo Fisher Scientific; Mississauga, ON, Canada) and purified using RNeasy micro kits (Qiagen, Valencia, CA, USA), including DNase digestion. Isolated RNA was stored at −20ºC for short-term storage prior to quantitation.

2.9 | RT-qPCR array

To assess cell-intrinsic differences between FACS-sorted FLP and FLN fibroblasts during homeostasis and wound healing, a RT^2 profiler array for genes associated with fibrosis (Qiagen; PAMM-120Z; Montreal, QC, Canada) was used to measure gene expression. Samples from four groups (FLP wound, FLN wound, FLP unwounded, FLN unwounded) were collected independently from eight mice. Isolated RNA was converted to cDNA with a RT^2 first strand kit (Qiagen), and pre-amplified with array-specific primers. Genes that were not consistently amplified in any group were removed

from further analysis. These removed genes included: *ccl12*, *ccr2*, *fasl*, *ifng*, *il13*, *il4*, *il5*, *inhbe*, *plg*, and *serpina1a*. Expression was normalized to a panel of housekeeping genes. Outliers in the $2^{-\Delta Ct}$ values were calculated using the ROUT method (Q = 1.0%)[24] in GraphPad Prism. Two groups of the 32 total groups were deemed to have a high number of outliers and were completely removed from further analysis. In the remaining data set, 23 data points were removed as outliers, of the 2,220 total data points remaining (~1%). Next, $2^{-\Delta Ct}$ values were compared using mixed effects models for each gene where cell lineage (FLP vs. FLN), or tissue type (Wounded vs. Unwounded) were included as fixed effects and mouse identification was included as a random effect using the "nlme" package[25] in R statistics software.[26] To correct for multiple comparisons, a false discovery rate correction set to 10% was used to identify differentially expressed genes.

2.10 | TaqMan® qPCR

To assess whether the expression patterns of wounded fibroblasts could be simulated by naïve fibroblasts in an in vitro system, a subset of genes of interest from the array were assayed using TaqMan® qPCR probe sets (Thermo Fisher Scientific; Mississauga, ON, Canada). Freshly sorted FLP and FLN fibroblast populations from naïve mouse skin, along with the two populations cultured in collagen gels for 7 days, were included and gene expression was assessed with TaqMan® probe sets using iTaq Universal 1-step master mix (Bio-Rad; Mississauga, ON, Canada) as per the manufacturer's instructions. The TaqMan® probe sets used in this study are listed in Table 2. Samples were run in triplicate. Threshold cycles were compared to a standard curve generated from serial dilutions of unsorted dermal isolates for relative quantitation. The resultant relative quantities were then normalized to endogenous 18S rRNA. Isolated cells from a total of six independent digestions, each combining the pooled fibroblasts from 4 to 6 mice, were assessed.

2.11 | Dorsal/ventral fibroblast isolation and flow cytometry

Dorsal and ventral skin were isolated from eight mice and dermal fibroblasts were isolated as described above for naïve dorsal skin, with the exception that the initial digestion with trypsin and dispase was excluded. The remaining isolated population was labeled with LIVE/DEAD fixable aqua, and antibodies for CD31 (APC), CD45 (APC), and EpCAM (APC) as described previously. Additionally, antibodies for PDGFRα (APC-eFluor780; Invitrogen), and CD26 (FITC; BioLegend; San Diego, CA, USA) were added 1:50 in PBS with 5% of FBS. Flow cytometry was performed using a LSRII cytometer as follows: Forward- and side-scatter were first used to select individual cells. Using a 405 nm laser with a 525/50 filter, cells negative for the LIVE/DEAD fixable aqua stain were selected. Next, using a 640 nm laser with 670/30 filter, cells negative for CD31, CD45, and EpCAM were selected. The remaining fibroblast populations were then stratified based on PDGFRα expression using the 640 nm laser with a 780/60 filter. The proportions expressing tdTomato and CD26 were then measured using the 561 nm laser with 610/20 filter, or the 488 nm laser with 530/30 filter, respectively.

TABLE 2 TaqMan® probes used to assess gene expression

Target	Probe ID
Acta2	Mm01546133_m1
Col1a1	Mm00801666_g1
Col3a1	Mm01254476_m1
Ctgf	Mm01192933_g1
Itga2	Mm00434371_m1
Itgb8	Mm00623991_m1
Lox	Mm00495386_m1
Mmp3	Mm00440295_m1
Dlk1	Mm00494477_m1
Dpp4	Mm00494548_m1
Pdgfra	Mm00440701_m1
Thy1	Mm00493681_m1
Eukaryotic 18S	4332641

2.12 | Ventral wound healing

To investigate differences in FLP fibroblast content between dorsal and ventral wounds following injury, 4 mm circular excisional wounds were produced in the dorsal and ventral skin within the same individual mice. Mice were anesthetized using isoflurane (5% induction; 2% maintenance), and the dorsal and ventral skin were shaved and treated with depilating cream. The wounds were made along a similar axial plane at the level of the thorax. Two 4 mm ventral, and two 4 mm dorsal wounds were created using a biopsy punch. The wounds were not splinted or bandaged to minimize stress on the animals. Following surgery, pain was controlled using 0.05 mg/kg buprenorphine delivered intraperitoneally prior to surgery, 6–8 hours following surgery, and daily thereafter for 3 days. Images were taken over the course of healing and wound sizes were measured digitally. To reduce the risk of infection of ventral wounds, mice were housed on absorbent padding. No signs of infection were noted. Dorsal and ventral wounds were created in eight mice, with four mice euthanized at each of 7 and 14 days post wounding. Wound tissue was collected for histological analysis to assess FLP content.

2.13 | Statistical methods

With the exception of the analysis performed on the array data as described in detail above, statistical analyses were performed using R statistics software [26] using the "lme4" package for linear and nonlinear mixed effects models,[27] and the "multcomp" package for simultaneous inference in general parametric models.[28] GraphPad Prism software version 6 (GraphPad, La Jolla, CA) was used to produce graphs. Statistical analyses were performed using linear mixed effects models or *t*-tests where appropriate. For linear mixed effects models, multiple comparisons were corrected as described by Hothorn et al. (2008). For multiple *t*-tests, multiple comparisons were corrected using a Bonferroni method. Corrected *p*-values < 0.05 were considered to be statistically significant.

3 | RESULTS

3.1 | *Foxd1* was expressed during murine embryonic development

To first explore the contribution of *foxd1*-expressing dermal progenitors to murine skin development, embryonic tissues were investigated using a lineage tracing strategy to track *foxd1*-derived populations as well as cells with an active *foxd1* promoter (schematic shown in Figure 1A). These populations were observed to contribute to the dermis during early development (Figure 1B). More specifically, through assessment of *foxd1* promoter activity in embryos from E9.5 to E17.5, an active promoter was noted from E9.5 to E11.5 within the head and in the dorsal region of the embryo, where it was active in cells in proximity to the neural tube, both ventrally and laterally. At E14.5, the promoter remained active within the head, but reduced expression was noted moving posteriorly. No *foxd1* promoter activity was detected at E17.5.

Notably, at E9.5, the earliest stage examined, tdTomato-positive (*foxd1*-lineage positive; FLP) cells that were GFP-negative were present within the most dorsal tissue of the embryo, suggesting they were derived from a population that expressed *foxd1* prior to E9.5. By E14.5 and up to the final stage examined of E17.5, it was observed that FLP cells contributed to the cell populations within the dermis (Figure 1B). FLP cells were also evident in several internal organs throughout the embryo, including, but not limited to, the kidney, lungs, and with a low frequency in the heart (Figure S1).

Next, an mTmG reporter system (schematic shown in Figure 2A) was used to clearly label both FLP and FLN populations. Within the developing dermis, FLP cells were distributed primarily along the midline, dorsal to the neural tube, however, the frequency of these cells was decreased in the ventrolateral direction (Figure 2B–C). Within adult mice, FLP cells were abundant within the dorsal dermis, but only sparsely populated the ventral dermis (Figure 2D). Despite offering a

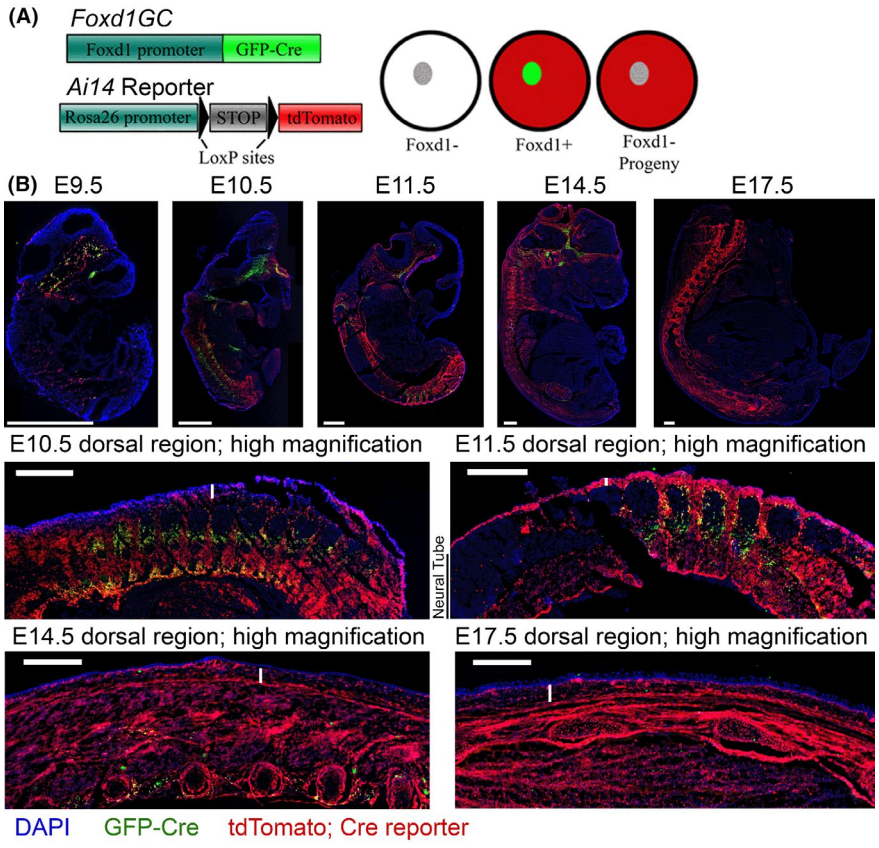

FIGURE 1 *Foxd1* is expressed by dorsal dermal fibroblast progenitors during embryonic development. (A) *Foxd1GC* mice were crossed with *Ai14* reporter mice to track *Foxd1*-expressing progenitors (green) and their progeny (red). (B) Using this reporter system, *Foxd1* expression was observed within the head and dorsal region in proximity to the neural tube. FLP cells (red) contributed to a range of tissues within the embryo, including the dermis. Scale bars in complete embryo cross sections indicate 1 mm, and in the magnified dorsal regions below indicate 500 μm. Vertical white bars indicate the approximate depth of the developing dermis in the high magnification images. For each time point, representative images are shown from three embryos

system that clearly distinguished between the FLP and FLN populations, a qualitative decrease in the frequency of FLP cells was noted with the mTmG reporter system compared to the *Ai14* reporter. Such findings have also been reported by others who have linked recombination efficiency to the length between *loxP* sites in various reporter strains.[29,30] Importantly, this issue is pronounced when Cre expression is low, suggesting that the *foxd1* promoter is active only briefly during development. Due to potential limitations of using this reporter to track all cells derived from *foxd1*-expressing progenitors, the *Ai14* reporter was used for the remainder of this study.

To further define when dermal FLP progenitors express *foxd1* during development, a tamoxifen-inducible system (*Foxd1GCE*/*Ai14*; schematic shown in Figure 3A) was utilized to induce recombination at specific intervals and investigate down-stream evidence of recombination within the dorsal skin (Figure 3B). While tamoxifen injection from E5.5 to E6.5 did not result in detectable recombination, injection at all other intervals spanning from E7.5 to E11.5 yielded tdTomato-positive FLP cells within the dorsal dermis at E14.5. Notably, a difference in the populations labeled between earlier (E7.5–8.5) and late (E10.5–11.5) tamoxifen injection was observed. More specifically, while recombined cells were identified throughout the developing dermis following earlier injection, later injection primarily labeled the more ventral cells in the developing dorsal dermis.

3.2 | *Foxd1*-expressing cells are rare in postnatal tissue during homeostasis and following wounding

In adult skin, FLP cells were present throughout the dermis and hypodermis, and following wounding, were observed

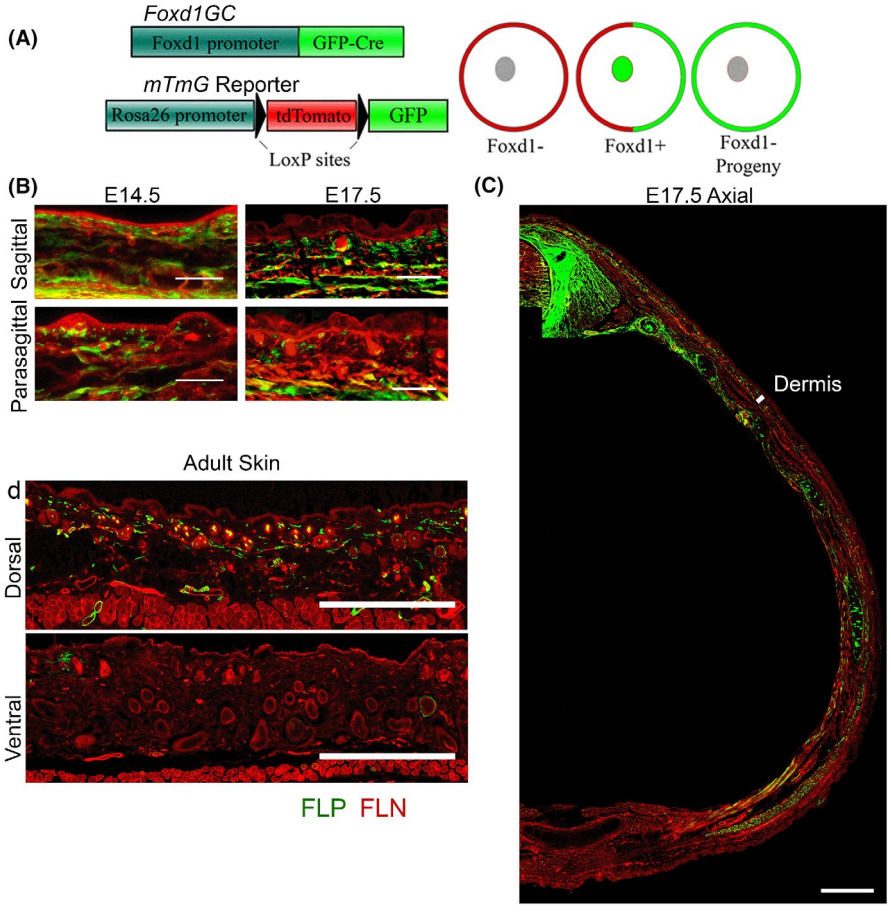

FIGURE 2 FLP cells primarily contribute to the dorsal dermis, with limited contribution to the ventral dermis during development and in adult tissue. (A) *Foxd1GC* mice were crossed with *mTmG* reporter mice to differentiate FLP (green) and FLN (red) populations. (B–C) During development, FLP fibroblasts were primarily localized to the midline in the dorsal dermis, decreasing in density in the ventrolateral direction. Scale bars indicate 200 μm for the sagittal and parasagittal cross sections, and 1 mm for the axial cross section. Representative images from five embryos are shown for the sagittal sections, and from three embryos for the axial sections. The dorsal midline is in the upper left corner of the axial images. (D) A similar distribution was also observed in adult tissue, where FLP fibroblasts were observed at high density in the dorsal skin, but were infrequent within the ventral skin. Scale bars indicate 1 mm. Representative images are shown from three adult mice

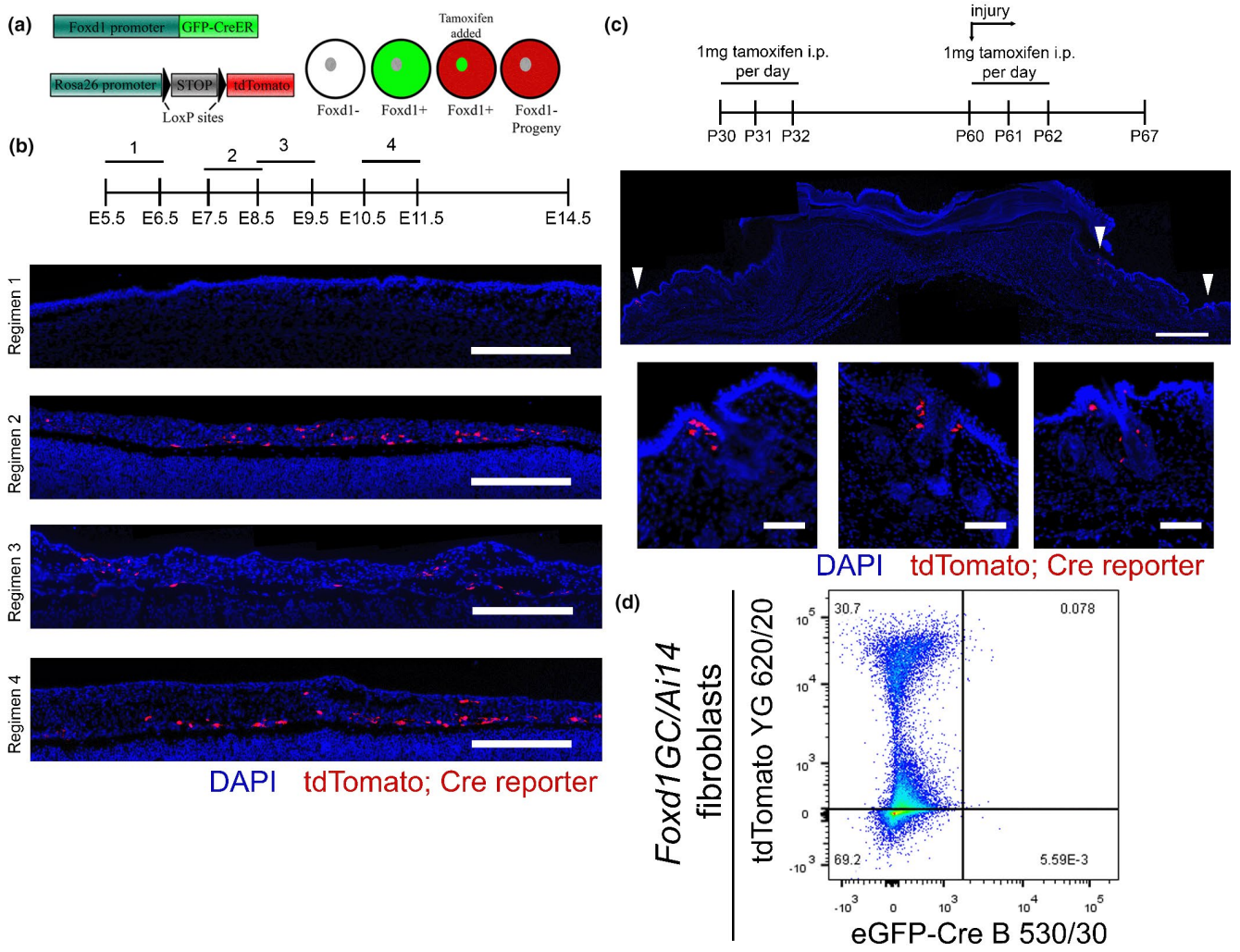

FIGURE 3 *Foxd1* is expressed primarily during development with limited detection observed in adult skin. (A) To further determine when FLP fibroblast progenitors expressed *Foxd1*, a tamoxifen inducible Cre model, *Foxd1GCE*, was explored in combination with an *Ai14* reporter. (B) Tamoxifen injection between embryonic days E7.5–E11.5 (regimens 2–4) resulted in recombination, yielding tdTomato FLP cells (red). Conversely, tamoxifen injection from E5.5–E6.5 (regimen 1) did not lead to recombination. Scale bars are 500 μm; a minimum of three embryos were observed for each injection regimen. (C) Tamoxifen injection in adult mice led to limited recombination, occurring only rarely in cells that were primarily associated with hair follicles. Arrows indicate recombination events, which are magnified in the panels below. Scale bars are 1 mm for the whole wound, and 100 μm in the magnified panels; postnatal injection of tamoxifen was performed in six mice. (D) To further explore whether the *Foxd1* promoter was active in adult mice, dorsal dermal fibroblasts were isolated from *Foxd1GC* mice crossed with *Ai14* reporter mice. Expression of the EGFP-Cre fusion protein was explored using flow cytometry. Flow cytometry was performed on a total of seven fibroblast isolations, 4–6 mice were used per isolation

in the granulation tissue. In rare cases, tdTomato$^+$ cells were also noted in the epidermis (data not shown); however, whether this was the result of nonspecific recombination, expression of *foxd1* by epidermal populations under specific conditions, or incidence of rare events of mesenchymal to epithelial transition is unknown. To determine if FLP cells were solely defined by embryonic *foxd1* expression, or if postnatal expression of *foxd1* also contributed to the FLP population, the tamoxifen inducible Cre model (*Foxd1GCE*/*Ai14*) was explored with adult mice. Additionally, as cutaneous wound repair relies on the reactivation of several pathways important for skin development,[31] activation of the *foxd1* promoter was queried following wounding using a non-splinted dorsal wound model. Using this system, tamoxifen was delivered to mice at 1 month of age and again after wounding at 2 months of age and a histological assessment of recombination was performed (Figure 3C). Wounded tissue and the surrounding skin were examined at 7 days post wounding during the proliferative phase of healing, characterized by dense fibroblast accumulation in this non-splinted model. Low numbers of cells in the skin and granulation tissue expressed tdTomato (<0.1%, $n = 6$). This was further supported using flow cytometry to detect GFP-Cre positive

fibroblasts in healthy adult skin of *Foxd1*GC/*Ai14* mice, in which a mean frequency of 0.076% (±0.043%; $n = 7$) GFP positive fibroblasts was measured (Figure 3D). Combined with the expression patterns observed during embryogenesis, these data suggest that the FLP cells present within the dermis were primarily derived from embryonic precursors that expressed *foxd1*, and that *de novo* expression of *foxd1* in postnatal dermis during homeostasis and wound healing was minimal, supporting that FLP cells represent a distinct lineage originating during embryogenesis.

3.3 | *Foxd1* lineage-positive cells contributed to diverse populations in adult skin

To characterize the differentiated populations within the skin derived from the *foxd1* lineage, the constitutively active *Foxd1*GC line crossed to the *Ai14* reporter was assessed. Within the dorsal skin, *foxd1*-derived populations were present throughout the dermis and within the panniculus carnosus muscle. To more specifically identify the populations these cells were contributing to within the dermis, sections of adult mouse skin were labeled with several markers expressed in fibroblasts (vimentin, PDGFRα, PDGFRβ, and CD26), the endothelial marker CD31, and the smooth muscle and myofibroblast marker αSMA. There were both tdTomato positive and tdTomato negative populations expressing each of the fibroblast markers explored (Figure 4A). In contrast, low overlap between tdTomato and CD31 was observed, suggesting that FLP cells were not a major contributor to the endothelial population within the dermis. Co-labeling with αSMA highlighted the contribution of FLP cells to arrector pili muscles, as well as some of the perivascular αSMA-expressing populations. Furthermore, FLP cells were observed in the dermal sheath population surrounding the hair follicles (Figure 4A, yellow arrows). The overlap between FLP cells and primarily fibroblast markers, associations with hair follicles, and contributions to arrector pili muscles fits with their presence within the early dermal tissues during development. Such early dermal progenitors have the potential to contribute to each of these populations.[3]

3.4 | *Foxd1* lineage-positive populations contributed to myofibroblasts during wound repair

Next, the contribution of FLP cells to wound healing was investigated using a splinted wound model in constitutively active *Foxd1*GC/*Ai14* mice. Samples were taken for histological analysis at 3, 7, 10, and 21 days post wounding (Figure 4B). At 3 days post wounding, sparse FLP cells were evident throughout the wound bed, with a qualitatively higher density observed at the wound edges. The density of FLP cells within the wound was qualitatively increased at 7 days post wounding and was further increased in the 10 day samples. The density appeared similar when comparing the samples at 10 and 21 days post wounding. The FLP cells within the wound tissue contributed to the stromal population, as shown by overlap of tdTomato with vimentin, PDGFRα, PDGFRβ, and CD26, as well as contributing to the αSMA positive myofibroblast population at day 3 and 10 post wounding (Figure 4C,D). However, it was evident that the FLP population only gave rise to a subset of these populations, with FLN cells also contributing. CD31 expression at day 3 was minimal beyond the edges of the wound, and again, overlap between tdTomato and CD31 was minimal, supporting that the *foxd1* lineage was not a major contributor to endothelial cells in the dermis.

3.5 | *Foxd1* lineage-positive fibroblasts did not mimic expression patterns of previously defined lineages

To determine if the FLP population overlaps with previously identified dermal fibroblast subpopulations, the expression of a set of markers was assayed in isolated FLP and FLN populations. Using FACS, a negative selection approach was taken, removing cells positive for EpCAM, CD45, or CD31, thereby enriching for the fibroblast population in naïve unwounded skin (Figure 5A). Notably, some of the cells excluded using this strategy did express tdTomato and thus could represent epithelial or endothelial populations that were not frequently observed histologically. Alternatively, these could also represent hematopoietic populations. The fibroblast enriched populations were then sorted into FLP and FLN populations based on their expression of tdTomato. Following isolation, the expression of fibroblast markers *dlk1*, *dpp4*, *pdgfra*, and *thy1* were assessed (Figure S2). Expression of *dlk1* and *dpp4* have been utilized to differentiate between previously identified fibroblast subsets, whereas *pdgfra* and *thy1* have been observed to be widely expressed across fibroblast populations.[2,3,11-13] Notably, cell lineage did not significantly affect the expression of any of these genes ($p > 0.05$).

3.6 | *Foxd1* lineage-positive fibroblasts displayed divergent fibrosis-related gene expression patterns during homeostasis and wound repair

Next, whether the *foxd1* lineage was associated with functional differences within the fibroblast population during homeostasis and following wounding was explored using gene

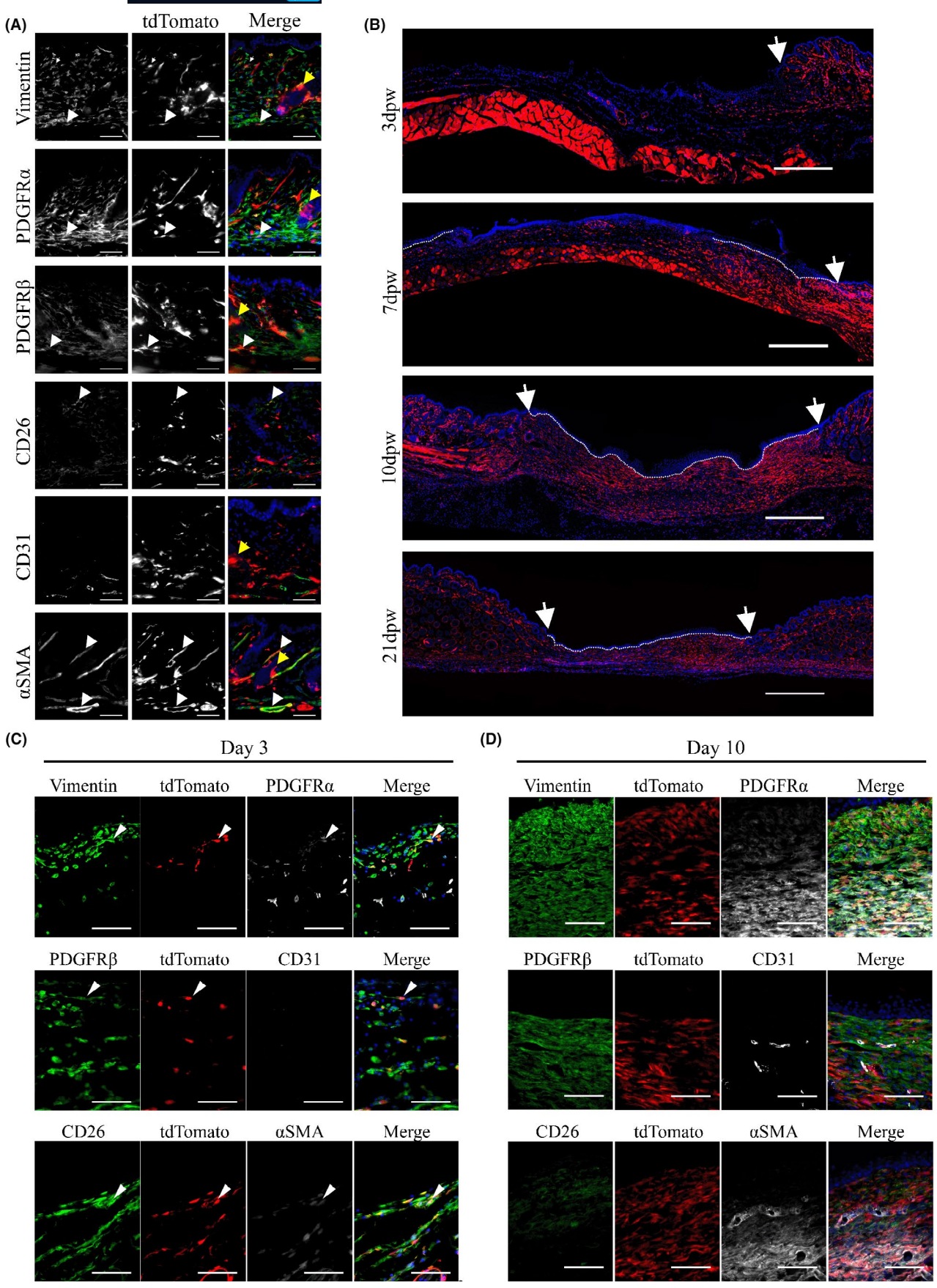
(A)
tdTomato
Merge
Vimentin
PDGFRα
PDGFRβ
CD26
CD31
αSMA
(B)
3dpw
7dpw
10dpw
21dpw
(C)
Day 3
Vimentin
tdTomato
PDGFRα
Merge
PDGFRβ
tdTomato
CD31
Merge
CD26
tdTomato
αSMA
Merge
(D)
Day 10
Vimentin
tdTomato
PDGFRα
Merge
PDGFRβ
tdTomato
CD31
Merge
CD26
tdTomato
αSMA
Merge

FIGURE 5 FLP fibroblasts and FLN fibroblasts contribute differentially to skin homeostasis and wound repair, but do not maintain their distinct characteristics following in vitro culture. (A) Fibroblasts were isolated from dorsal wounded and unwounded skin from *Foxd1GC/Ai14* mice 10-days post wounding ($n = 8$ mice) and from healthy naïve skin ($n = 9$ isolations; 4–6 mice per isolation) and enriched by FACS. (B) The fraction of cells derived from the *Foxd1* lineage within these populations was modestly greater in the wounded population compared to the healthy naïve population. Data were analyzed with linear mixed effects models; $^{*}p < 0.05$. (C and D) Isolated RNA from wounded and unwounded dermal fibroblasts was compared using Qiagen RT^2 Profiler arrays, and transcripts significantly enriched in either FLP (red) or FLN (green) populations are shown. Data were analyzed by multiple linear mixed effects models and were controlled for multiple comparisons using a false discovery rate correction of 10%. (E) Naïve FLP and FLN fibroblasts were isolated from the dorsal skin, and mRNA expression was compared following culture in 2 mg/ml collagen gels with or without treatment with 5 ng/ml TGFβ1 for 1 week. 18S rRNA was used to normalize expression. Dorsal skin was pooled from 4 to 6 mice for each isolation; data were pooled from six independent cell isolations. Data were analyzed with linear mixed effects models; $^{*}p < 0.05$; $^{**}p < 0.01$; $^{***}p < 0.001$

expression arrays. Wound tissue and unwounded skin surrounding the wound were isolated from constitutively active *Foxd1*GC/*Ai14* mice 10 days following wounding and sorted based on the FACS-based strategy described above. Based on the histological assessment of splinted wounds above, day 10 represented the time when fibroblasts were consistently present at high density within the central region of the wounds and would be expected to be actively synthesizing extracellular matrix to promote wound repair. No differences in the distribution of FLP fibroblasts were evident between wounded and unwounded populations (60.0 ± 9.7 vs. 54.1 ± 8.5% FLP positive in wounded and unwounded, respectively; $p > 0.05$; Figure 5B). However, a modest increase in FLP fibroblast frequency was observed in the wounded tissue when compared to naïve healthy dorsal skin taken from mice that had not been wounded (60.0 ± 9.7% vs. 49.6 ± 6.8; $p < 0.05$).

From these populations, the RNA was isolated and gene expression was assessed using a PCR array for a preselected set of fibrosis-related genes. Gene expression data were compared between lineages within tissue status (i.e., FLP wounded vs. FLN wounded) and between tissue status within lineages (i.e., FLP wounded vs. FLP unwounded) and differentially expressed genes were determined (Figure 5C,D, complete list of comparisons shown in Tables S1–S4). Interestingly, a difference in transcripts enriched in the FLP fibroblasts versus those enriched in FLN fibroblasts was noted. In general, the FLP fibroblasts from either wounded or unwounded tissue were enriched for transcripts associated with matrix production and remodeling, including *col1a2*, *col3a1*, *dcn*, *lox*, *mmp2*, *mmp3*, *mmp8*, *mmp14*, *serpinh1*, and *timp2*, as well as transcripts for signaling proteins involved in matrix regulation including *ctgf*, *tgfb2*, *tgfb3*, *and thsp2*. In contrast, the FLN population was enriched in transcripts associated with cell-cell (*bmp7*, *edn1*, *il1a*, *pdgfb*, *tnf*) and cell-matrix (*itga2*, *itga3*, *itgb6*, *itgb8*) interactions.

3.7 | Fibroblast lineage-specific differences were not maintained in culture

To determine whether these populations could be further investigated in a controlled culture environment, the effect of culturing on gene expression patterns in cells derived from healthy, naïve dermis from mice that were not wounded was explored. Using a type I collagen gel as a compliant three-dimensional culture substrate, mRNA levels of a selection of candidate genes identified on the array were assessed in FACS-sorted naïve, healthy dorsal dermal fibroblasts directly following isolation (baseline), and again after 1 week in culture in the presence or absence of TGFβ1 (Figure 5E). Importantly, in this model, significant differences between cell lineages were only noted in the baseline populations for *col1a1*, *col3a1*, and *itgb8* ($p < 0.05$). No differences were noted between the FLP and FLN lineages following 1 week of culture under the conditions in the current study.

3.8 | Ventral skin has reduced FLP content during homeostasis and following wounding

From our previous histological analysis, it was evident that the ventral skin contained a greatly reduced frequency of FLP fibroblasts (Figure 2D). To confirm this finding and quantitatively assess fibroblast marker expression, naïve ventral and dorsal skin were isolated and cells were extracted for flow cytometry. After selecting fibroblasts based on negative expression of CD31, CD45, and EpCAM, cells were stratified based on their expression of PDGFRα, tdTomato, and CD26 (Figure 6A–B; Figure S3). The frequency of PDGFRα expressing cells was similar between the dorsal and ventral skin, as was the frequency of $CD26^{+}$ cells. In contrast, as observed histologically, tdTomato expression, associated with FLP fibroblasts, was significantly reduced within the ventral skin. To determine if FLP cells were recruited or if they preferentially expanded during wound repair in the ventral skin, pilot studies were performed using a new model in which both dorsal and ventral wounds were created in mice. Without precedent for performing these experiments, a minimally invasive excisional model without splinting was used. Histological analysis revealed that ventral wounds healed with a greatly reduced abundance of FLP cells compared to dorsal wounds (Figure 6C). In fact, the ventral wounds healed significantly faster than those in the dorsal skin (Figure 6D–E). However, it should be noted that mouse

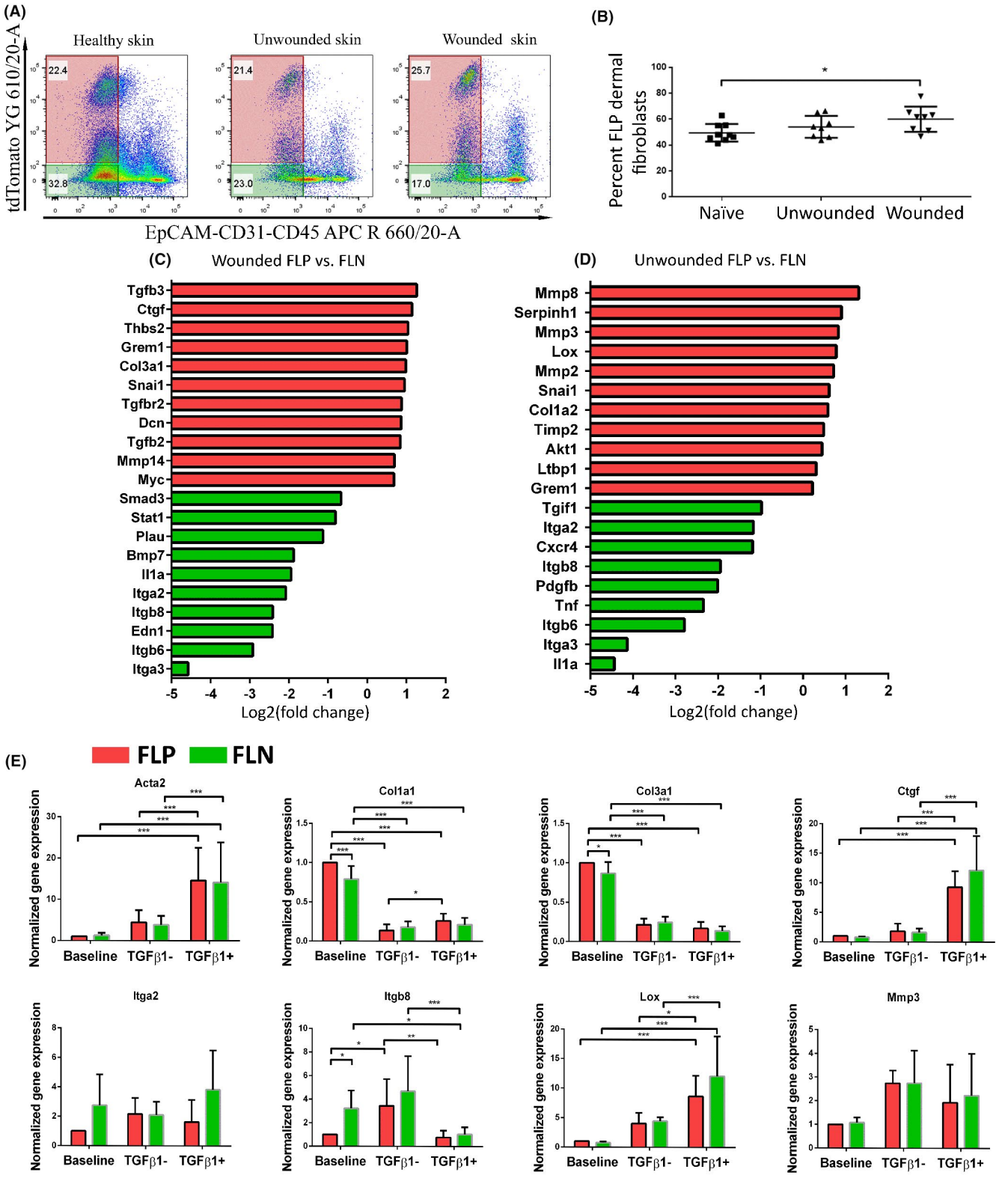

wound closure is largely influenced by contraction.[32] Thus, without wound splinting, these differences may simply be due to unique positional mechanics rather than changes to the granulation tissue. Taken together, these findings suggest that, at minimum, the FLP population is not required at high frequency for ventral wound repair.

4 | DISCUSSION

Using a lineage tracing approach, embryonic progenitors that differentially expressed *foxd1* were investigated and found to give rise to fibroblasts in adult tissue that uniquely contributed to skin homeostasis and wound repair. While this

FIGURE 4 FLP cells contribute to diverse populations within the adult dorsal dermis, and to myofibroblasts upon wounding. Unwounded and wounded adult dorsal dermal tissues were isolated from *Foxd1GC/Ai14* mice. (A) In unwounded dorsal skin, FLP cells were observed to express markers associated with fibroblasts, perivascular cells, and arrector pili populations. Merged images show the marker of interest in green, tdTomato (FLP) in red and nuclei are labeled with DAPI in blue. Scale bars are 100 μm. White arrows indicate representative cells with dual labeling; yellow arrows highlight FLP populations associated with hair follicles. Representative images are shown from three mice. (B) FLP cells began to appear at 3 days post wounding (dpw) at the wound edge (indicated with arrows) and increased in density over time to 10 days post wounding, remaining up to 21 days post wounding. Underlying skeletal muscle, labeling positive for the *foxd1* lineage, was extracted along with the samples at 3 and 7 days post wounding to support the granulation tissue for processing. The panniculus carnosus muscle does not appear within the wound bed as it is cleaved during wounding. Dotted lines indicate the granulation tissue-epidermal junction. Scale bars are 1 mm; $n = 3$–4 mice per time point. (C and D) FLP cells within day-3 and day-10 granulation tissue co-labeled with fibroblast markers. Arrows indicate points of interest, highlighting overlap with fibroblast markers and FLP cells. Day 3 wounds were taken near the edge of the wound where most of the FLP cells were identified. Nuclei are stained with DAPI (blue). Scale bars are 100 μm. Representative images are shown from a sample of three mice at day 3 and 4 mice at day 10

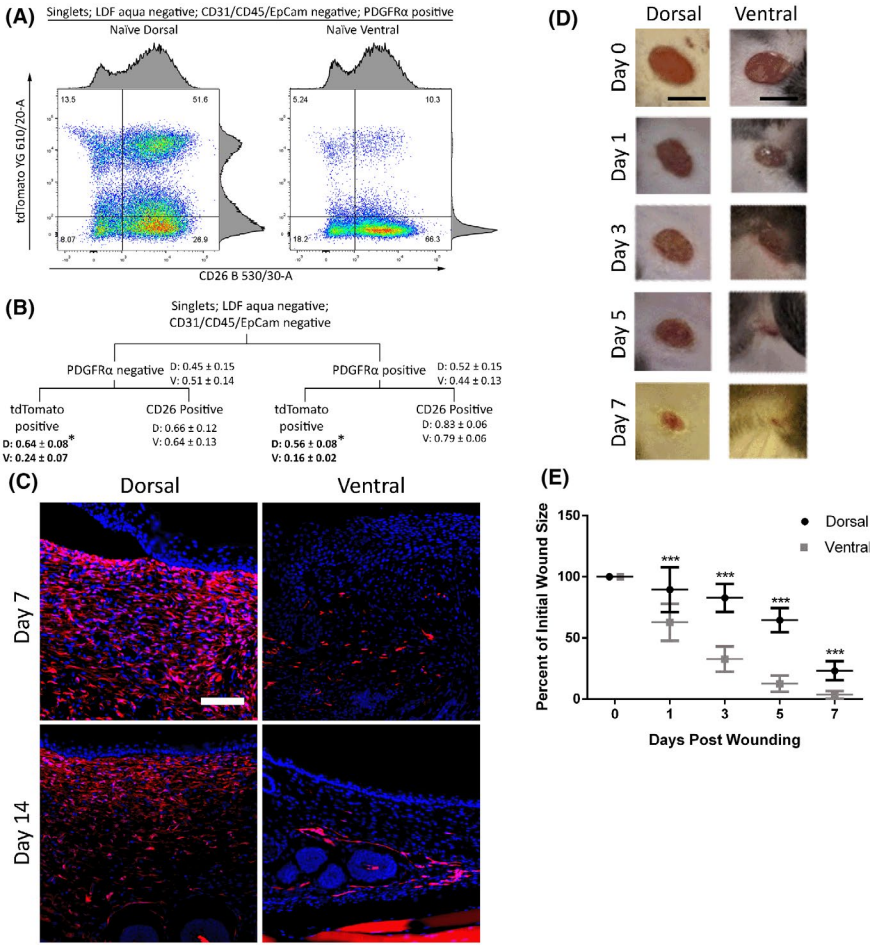

FIGURE 6 Ventral skin has reduced frequency of FLP fibroblasts during homeostasis and following wounding compared to dorsal skin. (A and B) Skin isolates were prepared from dorsal and ventral skin of *Foxd1GC/Ai14* mice and probed for the fibroblast markers PDGFRα and CD26, along with tdTomato expression as a marker of the *Foxd1* lineage. The frequency of FLP cells was significantly reduced within the ventral skin, however, the abundance of PDGFRα$^+$ and CD26$^+$ fibroblasts were similar in both regions. Skin isolates were collected from eight mice. Data were compared using multiple paired *t*-tests controlling for multiple comparisons with a Bonferroni correction. Bolded comparisons were significantly different between dorsal and ventral skin. *$p < 0.001$. (C) The frequency of FLP fibroblasts was reduced in ventral wound tissue relative to dorsal wound tissue at both 7- and 14-days post wounding. Wound tissue was collected from four mice at each 7- and 14-days post wounding. Scale bar indicates 100 μm. (D–E) Wound closure was significantly delayed in dorsal wounds compared to ventral wounds. Scale bars represent 4 mm; ***$p < 0.001$

lineage appears to have an important role in matrix remodeling, it is evident that ventral wound repair occurs with a greatly reduced frequency of *foxd1*-lineage-positive cells. Although it has previously been hypothesized that fibroblasts differentiate into distinct and stable populations that have characteristic functions,[33,34] these data expand upon

this notion and support more recent studies showing that, in fact, these different fibroblast populations arise from unique embryonic progenitors.[2,3] In contrast, our novel findings in ventral skin support the possibility that fibroblast populations derived from unique embryonic progenitors may undergo convergent differentiation to give rise to fibroblasts with similar functionality.

Interestingly, the FLP population described here does not directly overlap with distinct embryonic lineages that have been previously identified within the skin in murine models. For example, the *engrailed-1* lineage described in adult mice by Rinkevich et al. (2015) and during development by Jiang et al. (2018), has some similarities with the *foxd1* lineage, but also exhibits differences. Similar to the *foxd1* lineage, Jiang et al. described a developmental migratory pattern in which progenitors located ventral and lateral to the neural tube migrated into the medial dorsal dermis around E10.5, and then, began to spread laterally.[35] However, the *foxd1* lineage represented only ~50% of the dermal fibroblasts in adult unwounded tissue, in comparison to ~70% described for the *engrailed-1* lineage by Rinkevich et al. (2015). Further, differential gene expression of *dpp4* was not detected in the *foxd1* lineage, which was upregulated at the protein level in the *engrailed-1* lineage. Regardless, both *foxd1*- and *engrailed-1*-derived populations display an enhanced fibrogenic potential compared to their lineage-negative counterparts, and thus, likely share a common subset of cells specialized in matrix production.

The populations described by Driskell et al. (2013) showed distinct spatial separation between the papillary and reticular dermis during development and early postnatal growth, which was not identified in the *foxd1* lineage in either embryonic or adult tissues. Moreover, differential gene expression of *dlk1* and *dpp4*, which correspond with the reticular and papillary dermal fibroblast populations, respectively, was not evident in the populations sorted based on the *foxd1* lineage. Interestingly, the differentiation of multipotent progenitors into upper and lower dermal lineages described by Driskell et al. occurs around E12.5, which is later than the expression observed for *foxd1*. Further, in the inducible Cre model described here, later tamoxifen injection from E10.5 to E11.5 yielded recombination primarily in the more basal fibroblast population by E14.5, whereas earlier injection resulted in a more widely distributed population of recombined cells, spread between the basal and superficial populations. Thus, it is proposed that as cells migrated dorsally into the dermis during development, they ceased to express *foxd1*.

In this proposed model, the cells that migrate earlier in development would stop expressing *foxd1* earlier and become the most dorsal fibroblasts in the skin, whereas those migrating later would have more sustained *foxd1* expression and contribute more ventrally within the dermis. The significance of this is that the multipotent progenitors described at E12.5 by Driskell et al. could already be predetermined upper or lower dermal populations based on positional cues which arise from a temporal switch related to their initial migration into the developing dermis. Moreover, the observed stratification of the labeled population based on the timing of tamoxifen injection, when combined with the work of Driskell et al., suggests that a sub-lineage of FLP fibroblasts are reticular FLP fibroblasts, which may be distinct from papillary FLP fibroblasts. As the reticular population was shown to be the primary contributor to granulation tissue formation and matrix deposition,[3] it would be expected that a reticular FLP lineage may be a more specific fibrogenic population of interest. Unfortunately, due to complications with tamoxifen injection into pregnant females, a dose that yielded high levels of recombination and resulted in live births was not identified, and thus, this was not pursued further. However, it is speculated based on the tissue architecture during early repair, as well as from the findings of Driskell et al., that the FLP fibroblasts that migrated into the wound were coming from the lower dermis, and thus, the repair process was selecting for this reticular subpopulation.

Although *foxd1* provided a useful lineage marker, its functional role during skin development is uncertain. A recent study highlighted a role of *foxd1*-expressing cells in hair follicle formation, with expression noted at E15.0.[36] The findings presented here support these data, with FLP cells observed in proximity to hair follicles during development and in adult tissue within the dorsal region. However, it is apparent that *foxd1* is also expressed prior to hair follicle development in a subset of fibroblast progenitors. Deletion of *foxd1* during development has previously been observed to impair kidney development.[16] It was determined that *foxd1* was necessary for appropriate differentiation of renal progenitors, in part by inhibiting decorin expression, resulting in enhanced BMP signaling. As the majority of ventral fibroblasts are derived from FLN progenitors, it seems unlikely that *foxd1* is required for skin development, but investigation of its function may provide insight into potential differences between dorsal and ventral skin and its initial patterning.

Using histological and gene expression analyses, expression of α-SMA was consistent in both cell lineages within the wound, suggesting that myofibroblast activation was similar in both groups. Conversely, the differential gene expression patterns suggest that while both groups can differentiate into a contractile myofibroblast phenotype, their complementary functional specification may be diverse. Importantly, unique expression signatures were noted suggesting that the expression of genes associated with matrix synthesis and remodeling was enhanced in FLP fibroblasts, while the expression of genes associated with cell signaling was enhanced in FLN fibroblasts. In general, it is notable that the gene expression changes, especially those upregulated in the FLP subset, were subtle, with both populations producing transcripts for

ECM synthesis and remodeling. Whether a depletion of this population would result in reduced collagen production, or whether FLN cells could compensate for this loss, would require further investigation. Studies of the greater fibrogenic *engrailed-1* lineage using diphtheria toxin-induced depletion or selective cell transplantation in wound healing models have shown that the extent of scar tissue formation is directly linked to the relative abundance of this population.[2,35] Consequently, it would be interesting to explore the *foxd1* lineage in these model systems, as it would be postulated to have similar functional effects.

Due to the enrichment of transcripts for cell receptors and signaling molecules in the FLN population, it was proposed that these cells may act as regulators of FLP function. However, in order to systematically explore the interactions between the two populations, a robust in vitro model system would be required. It is well established that culture on stiff substrates results in myofibroblast activation.[7,37] Conversely, culture on compliant 3D matrices can yield a quiescent, nonproliferative cell state that more closely mimics that of native tissue.[38,39] To first determine if gene expression could be maintained in vitro, a compliant collagen gel was used as a culture substrate and TGFβ1 was used to selectively stimulate myofibroblast activation. Naïve fibroblasts were used rather than the unwounded and wounded populations due to the cell yield required. Using this strategy, expression of *col1a1*, *col3a1*, and *itgb8* integrin were determined to be significantly affected by cell lineage in this freshly isolated population, similar to the array findings. However, it is notable that the gene expression differences in the naïve healthy population appeared to be diminished relative to the fibroblasts isolated from unwounded tissue from mice 10 days post wounding that were included in the array analysis, suggesting that the unwounded cells may have been in a more "activated" state due to a systemic response to the wounds.

Unfortunately, culturing isolated naïve fibroblasts on collagen gels resulted in a loss of their distinct phenotypes. For example, genes that were differentially expressed between lineages upon isolation, including *col1a1*, *col3a1*, and *itgb8*, were expressed similarly between the groups after culturing. It is well established that culture on collagen gels reduces collagen synthesis,[40,41] which occurs through α1β1 integrin stimulation.[42] Treatment with TGFβ1 was sufficient to upregulate *col1a1* expression in FLP fibroblasts, albeit to a level below that of freshly isolated fibroblasts. In partial contrast to these findings, after culturing human papillary and reticular dermal fibroblasts on tissue culture plastic, Philippeos et al. found that while the populations did not retain their native differential expression of Wnt-signaling-related genes, they maintained differences in the expression of inflammatory mediators and ECM-related genes including *col1a1* and *col1a2*.[12] Moreover, in an organotypic culture system comprised of decellularized human skin seeded with a keratinocyte layer and cultured human fibroblasts from either the papillary or reticular dermal populations, both fibroblast populations maintained functional differences.[12] Potentially, an organotypic culture system as employed by Philippeos et al. could be useful to study cell function in a more biologically relevant model.

From this work, it is evident that within the dorsal skin, FLP and FLN fibroblasts are both capable of producing αSMA to contribute to activated myofibroblasts during tissue repair. However, it is also apparent that they have unique specializations and potentially work together in concert during homeostasis and repair. Further exploration of the interaction between these fibroblast subsets is warranted to uncover these mechanisms. Building from this work, a possible model for the interaction of FLP and FLN populations is one in which the FLP cells specialize as a matrix secreting population, whereas the FLN cells play a more supportive role, sensing the ECM through integrin receptors and regulating the FLP population through cytokine secretion to promote tissue repair.

Finally, as it was hypothesized that cell lineage was a predictor of cell phenotype, wound healing within ventral skin, which has a unique embryonic derivation to dorsal skin, was explored. The ventral dermis derives from the lateral plate mesoderm, whereas dorsal dermis derives from the paraxial mesoderm.[43,44] Importantly, it was observed that *foxd1*-expressing progenitors primarily contributed to the dorsal, but not ventral dermis. Although these regions had disparate developmental origins, the relative frequencies of cells expressing the functional fibroblast markers PDGFRα and CD26 were similar between the dorsal and ventral skin. Further, upon wounding, there was no obvious selective expansion of the FLP population, suggesting that ventral skin heals normally with a greatly reduced FLP frequency. These findings also align with those in human skin, where similar expression of fibroblast markers including CD26 was noted in different regions including the abdomen, back, thigh, and arm.[12] In contrast to these similarities, dorsal skin and oral mucosa have been noted to have unique fibroblast populations in mice, with the dorsal skin having more fibrotic fibroblast populations.[2]

To our knowledge, lineage tracing of fibroblast populations in ventral skin has not previously been explored, however, this creates a unique opportunity to begin to investigate differences in highly similar tissues arising from distinct embryonic progenitors. From the initial findings reported here, it seems that unique lineages can yield similar fibroblast phenotypes. Thus, even though lineage can account for functional differences within a tissue site, it is not sufficient to predict phenotypes across tissue locations. Perhaps, as noted here and by others,[35] embryonic lineage is a predictor of developmental migratory patterns, leading to unique spatial localization, which in turn creates unique

positional cues controlling cell fate. This model is in line with the findings of others reporting spatially distinct fibroblast phenotypes within tissues.[3,12,45] Moreover, this would better account for the similarities between dorsal, ventral, and perhaps other regions of skin that cannot be explained due to embryonic derivation. Further temporal analysis of fibroblast populations in different regions is also required to assess whether the noted phenotypic convergence between different regions occurs during development or postnatally. While fibroblasts undergo considerable change developmentally,[3,35] Shook et al. (2018) observed reduced fibroblast heterogeneity in the dorsal skin of aged mice relative to young mice, suggesting that these populations are constantly changing.[46] Similarly, whether different skin regions age at different rates is not well characterized but could have important implications for therapeutic development.

In the present study, *foxd1* expression by embryonic progenitors enabled the tracking of distinct fibroblast lineages that maintained functional differences into adulthood. Overall, this work further supports the use of fibroblast lineage as a predictor of cell function, but highlights that this is likely only true within a given tissue site. In fact, lineage itself may simply predict a cell's location, which in turn defines its phenotype. This interrelationship between the cell-intrinsic control over fate as a function of fibroblast lineage, and the cell-extrinsic control over fate as a function of the fibroblast's microenvironment still needs further exploration. Comparative analysis between ventral and dorsal skin offers a unique strategy to begin to elucidate these relationships.

ACKNOWLEDGMENTS

We would like to thank Dr. Kristin Chadwick at the London Regional Flow Cytometry Facility for her technical expertise with the FACS experiments. Work was funded by the Canadian Institutes of Health Research Operating grant (Grant no: 326100) to DWH. JTW was the recipient of a Natural Sciences and Engineering Research Council of Canada Alexander Graham Bell Scholarship.

CONFLICTS OF INTEREST

The authors declare no conflicts of interest.

AUTHOR CONTRIBUTIONS

J. Walker, L. Flynn, D. Hamilton designed research; J. Walker performed research; J. Walker analyzed data; J. Walker, L. Flynn, D. Hamilton wrote the paper.

ORCID

Douglas W. Hamilton https://orcid.org/0000-0002-9798-5197

REFERENCES

1. Singer AJ, Clark R. Mechanisms of Disease - Cutaneous Wound Healing. *N Engl J Med*. 1999;341:738-746.
2. Rinkevich Y, Walmsley GG, Hu MS, et al. Identification and isolation of a dermal lineage with intrinsic fibrogenic potential. *Science*. 2015;348:aaa2151.
3. Driskell RR, Lichtenberger BM, Hoste E, et al. Distinct fibroblast lineages determine dermal architecture in skin development and repair. *Nature*. 2013;504:277-281.
4. Suga H, Rennert RC, Rodrigues M, et al. Tracking the elusive fibrocyte: Identification and characterization of collagen-producing hematopoietic lineage cells during murine wound healing. *Stem Cells*. 2014;32:1347-1360.
5. Dulauroy S, Di Carlo SE, Langa F, Eberl G, Peduto L. Lineage tracing and genetic ablation of ADAM12 + perivascular cells identify a major source of profibrotic cells during acute tissue injury. *Nat Med*. 2012;18:1262-1270.
6. Marangoni RG, Korman BD, Wei J, et al. Myofibroblasts in murine cutaneous fibrosis originate from adiponectin-positive intradermal progenitors. *Arthritis Rheumatol*. 2015;67:1062-1073.
7. Hinz B. Formation and function of the myofibroblast during tissue repair. *J Invest Dermatol*. 2007;127:526-537.
8. Gabbiani G. The myofibroblast in wound healing and fibrocontractive diseases. *J Pathol*. 2003;200:500-503.
9. Hu MS, Moore AL, Longaker MT. A Fibroblast Is Not a Fibroblast Is Not a Fibroblast. *J Invest Dermatol*. 2018;138:729-730.
10. Driskell RR, Watt FM. Understanding fibroblast heterogeneity in the skin. *Trends Cell Biol*. 2015;25:92-99.
11. Abbasi S, Sinha S, Labit E, et al. Distinct Regulatory Programs Control the Latent Regenerative Potential of Dermal Fibroblasts during Wound Healing. *Cell Stem Cell*. 2020;27:396-412.e6.
12. Philippeos C, Telerman SB, Oulès B, et al. Spatial and Single-Cell Transcriptional Profiling Identifies Functionally Distinct Human Dermal Fibroblast Subpopulations. *J Invest Dermatol*. 2018;138:811-825.
13. Tabib T, Morse C, Wang T, Chen W, Lafyatis R. SFRP2/DPP4 and FMO1/LSP1 define major fibroblast populations in human skin. *J Invest Dermatol*. 2018;138:1-9.
14. El Agha E, Kramann R, Schneider RK, et al. Mesenchymal Stem Cells in Fibrotic Disease. *Cell Stem Cell*. 2017;21:166-177.
15. Hinz B, Phan SH, Thannickal VJ, et al. Recent developments in myofibroblast biology: Paradigms for connective tissue remodeling. *Am J Pathol*. 2012;180:1340-1355.
16. Fetting JL, Guay JA, Karolak MJ, et al. FOXD1 promotes nephron progenitor differentiation by repressing decorin in the embryonic kidney. *Development*. 2014;141:17-27.
17. Levinson RS. Foxd1-dependent signals control cellularity in the renal capsule, a structure required for normal renal development. *Development*. 2005;132:529-539.
18. Humphreys BD, Lin S-LL, Kobayashi A, et al. Fate tracing reveals the pericyte and not epithelial origin of myofibroblasts in kidney fibrosis. *Am J Pathol*. 2010;176:85-97.
19. Hung C, Linn G, Chow Y-HH, et al. Role of lung Pericytes and resident fibroblasts in the pathogenesis of pulmonary fibrosis. *Am J Respir Crit Care Med*. 2013;188:820-830.
20. Feil S, Valtcheva N, Feil R. Inducible Cre Mice. In: Wurst W, Kühn R, eds. *Gene Knockout Protocols*, (2nd edn). Totowa, NJ: Humana Press; 2009:343-363.

21. Metzger D, Chambon P. Site- and time-specific gene targeting in the mouse. *Methods*. 2001;24:71-80.
22. Elliott CG, Wang J, Guo X, et al. Periostin modulates myofibroblast differentiation during full-thickness cutaneous wound repair. *J Cell Sci*. 2012;125:121-132.
23. Dunn L, Prosser HCG, Tan JTM, Vanags LZ, Ng MKC, Bursill CA. Murine Model of Wound Healing. *J Vis Exp*. 2013;e50265.
24. Motulsky HJ, Brown RE. Detecting outliers when fitting data with nonlinear regression - A new method based on robust nonlinear regression and the false discovery rate. *BMC Bioinformatics*. 2006;7:1-20.
25. Pinheiro J, Bates D, R-core (2014) Linear and Nonlinear Mixed Effects Models.
26. R core team. *R: A language and environment for statistical computing*. Vienna, Austria: R Found. Stat. Comput; 2017.
27. Bates D, Mächler M, Bolker BM, Walker SC. Fitting linear mixed-effects models using lme4. *J Stat Softw*. 2015:67.
28. Hothorn T, Bretz F, Westfall P. Simultaneous inference in general parametric models. *Biometrical J*. 2008;50:346-363.
29. Álvarez-Aznar A, Martínez-Corral I, Daubel N, Betsholtz C, Mäkinen T, Gaengel K. Tamoxifen-independent recombination of reporter genes limits lineage tracing and mosaic analysis using CreERT2 lines. *Transgenic Res*. 2020;29:53-68.
30. Liu J, Willet SG, Bankaitis ED, Xu Y, Wright CVE, Gu G. Non-parallel recombination limits cre-loxP-based reporters as precise indicators of conditional genetic manipulation. *genesis*. 2013;51:436-442.
31. Bielefeld KA, Amini-Nik S, Alman BA. Cutaneous wound healing: Recruiting developmental pathways for regeneration. *Cell Mol Life Sci*. 2013;70:2059-2081.
32. Chen JS, Wong VW, Gurtner GC. Therapeutic potential of bone marrow-derived mesenchymal stem cells for cutaneous wound healing. *Front Immunol*. 2012;3:1-9.
33. Phipps RP, Penney DP, Keng P, et al. Characterization of Two Major Populations of Lung Fibroblasts: Distinguishing Morphology and Discordant Display of Thy 1 and Class II MHC. *Am J Respir Cell Mol Biol*. 1989;1:65-74.
34. McIntosh JC, Hagood JS, Richardson TL, Simecka JW. Thy1 (+) and (-) lung fibrosis subpopulations in LEW and F344 rats. *Eur Respir J*. 1994;7:2131-2138.
35. Jiang D, Correa-Gallegos D, Christ S, et al. Two succeeding fibroblastic lineages drive dermal development and the transition from regeneration to scarring. *Nat Cell Biol*. 2018;20:422-431.
36. Mok K-W, Saxena N, Heitman N, et al. Dermal Condensate Niche Fate Specification Occurs Prior to Formation and Is Placode Progenitor Dependent. *Dev Cell*. 2019;48:32-48.e5.
37. Balestrini JL, Chaudhry S, Sarrazy V, Koehler A, Hinz B. The mechanical memory of lung myofibroblasts. *Integr Biol*. 2012;4:410-421.
38. Erler JT, Weaver VM. Three-dimensional context regulation of metastasis. *Clin Exp Metastasis*. 2009;26:35-49.
39. Rognoni E, Pisco AO, Hiratsuka T, et al. Fibroblast state switching orchestrates dermal maturation and wound healing. *Mol Syst Biol*. 2018;14:e8174.
40. Gillery P, Leperre A, Coustry F, Maquart FX, Borel JP. Different regulation of collagen I gene transcription in three- dimensional lattice cultures. *FEBS Lett*. 1992;296:297-299.
41. Eckes B, Mauch C, Hüppe G, Krieg T. Downregulation of collagen synthesis in fibroblasts within three-dimensional collagen lattices involves transcriptional and posttranscriptional mechanisms. *FEBS Lett*. 1993;318:129-133.
42. Langholz O, Rockel D, Mauch C, et al. Collagen and collagenase gene expression in three-dimensional collagen lattices are differentially regulated by a1b1 and a2b1 integrins. *J Cell Biol*. 1995;131:1903-1915.
43. Gilbert SF. *Developmental Biology*, (6th edn). Sunderland (MA): Sinauer Associates; 2000.
44. Olivera-Martinez I, Thélu J, Teillet MA, Dhouailly D. Dorsal dermis development depends on a signal from the dorsal neural tube, which can be substituted by Wnt-1. *Mech Dev*. 2001;100:233-244.
45. Sorrell JM, Caplan AI. Fibroblast heterogeneity: More than skin deep. *J Cell Sci*. 2004;117:667-675.
46. Shook BA, Wasko RR, Rivera-Gonzalez GC, et al. Myofibroblast proliferation and heterogeneity are supported by macrophages during skin repair. *Science*. 2018;362(6417):eaar2971.

SUPPORTING INFORMATION

Additional supporting information may be found online in the Supporting Information section.

How to cite this article: Walker JT, Flynn LE, Hamilton DW. Lineage tracing of Foxd1-expressing embryonic progenitors to assess the role of divergent embryonic lineages on adult dermal fibroblast function. *FASEB BioAdvances*. 2021;3:541–557. https://doi.org/10.1096/fba.2020-00110